Journal of
Computational and Theoretical Nanoscience
Vol. 9, 1–6, 2012

Molecular Dynamics Study on ZnO Nanowires Mechanical Properties: Strain Rate, Temperature and Size Dependent Effects

Jing Guo[1, 2], Bin Wen[1, *], and Roderick Melnik[3, 4]

[1] State Key Laboratory of Metastable Materials Science and Technology, Yanshan University, Qinhuangdao 066004, China
[2] Technical Center, BenXi Iron and Steel (Group) Co., Ltd.
[3] M[2] NeT Lab, Wilfrid Laurier University, Waterloo, 75 University Ave. West, Ontario, Canada N2L 3C5
[4] BCAM, Bizkaia Technology Park, 48160 Derio, Spain

Using molecular dynamics simulations, strain rate, temperature, size and orientation dependent mechanical properties of zinc oxide (ZnO) nanowire are carried out with tensile loading. It is found that, for the same cross-sectional areas, strain rates have almost no effect on Young's modulus, provided strain rates are within the range from 0.001 to 0.03 ps^{-1}. Our calculated results have also demonstrated that, as temperature ranging from 200 K to 1600 K, ZnO nanowires' Young's modulus are all monotonically decreasing with increasing temperature. Furthermore, at the temperature of 300 K, yield strength, Young's modulus, fracture strength and fracture strain increase dramatically with increasing cross sectional area. It is also demonstrated that, with increasing cross sectional area, the Young's modulus of ZnO nanowires eventually approaching that of bulk single-crystal ZnO. Finally, orientation dependent ZnO mechanical properties of nanowires have been studied at 300 K.

Keywords: Mechanical Properties, ZnO Nanowires, Strain Rates, Size Effects, Temperature Dependent Properties, Orientation Dependent Properties, Molecular Dynamics, Atomistic Methods.

RESEARCH ARTICLE

1. INTRODUCTION

In the past years, semiconductor nanostructures have become the focus of intensive research owing to their unique properties and important applications in mesoscopic physics, biology and medicine, as well as fabrication of nanoscale electronic and photonic devices.[1, 2] In particular, as a typical semiconductor compound, zinc oxide (ZnO) has been receiving considerable attention due to its good optical, electrical, and piezoelectric properties.[3] In recent years, various functional ZnO nanostructures have been synthesized, such as very thin nanosheets,[4, 5] nanorings,[6] nanohelices,[7] nanobelts,[8–10] nanotubes,[11] nanowires[12, 13] and nanowire arrays etc.[14] Stimulated by the achieved experimental progress, a number of theoretical and experimental efforts have recently been carried out in order to better understand the properties of ZnO at the nanoscale.[15–17]

Since ZnO nanostructures have significant applications as active components in nanoelectromechanical systems,[18] the mechanical properties of ZnO nanostructures have been studied extensively for designing, manufacturing, and operating such devices. Recently, a number of theoretical and experimental efforts have been carried out. For example, for the phase stability of ZnO nanostructures under stress, calculations by Zhou et al. indicated that the uniaxial strain on ZnO nanowires along $[01\bar{1}0]$ can lead to the transformation from wurtzite (WZ) to an unbuckled WZ phase.[19, 20] As far as the Young modulus of ZnO nanostructures is concerned, there are still some contradictions between experimental and theoretical results. Indeed, several experimental measurements strongly indicated that the Young modulus of ZnO nanostructures is lower than 140 GPa for bulk ZnO.[21–26] However, other experimental[27] and theoretical results[19, 28, 29] indicated that the Young modulus of ZnO nanostructures is higher than that of bulk ZnO. In particular, it is also demonstrated that in contrast to recent reports, Young's modulus is essentially independent of diameter and close to the bulk value.[17] Therefore, the mechanical properties of ZnO nanostructures under the tensile loading need further clarification.

In this work, we address this issue by using Molecular Dynamics (MD) simulations to present an accurate

*Author to whom correspondence should be addressed.

 1546-1955/2012/9/001/006 doi:10.1166/jctn.2012.2629

description of the Young modulus and related mechanical properties of ZnO nanowires. In particular, the effects of strain rate, size, temperature and orientation on ZnO nanowires mechanical properties have been analyzed in detail.

2. COMPUTATIONAL METHOD

In this contribution, we consider [0001]-oriented wurtzite (WZ) ZnO nanowires (NWs) with hexagonal prism structures. The structures in Figure 1(a) are the top and side views of the initial WZ ZnO nanowires supercell, respectively. The nanowires are periodic in the c-direction but of finite extent in the section plane. We use periodic boundary conditions together with an in-plane lattice parameter to ensure there is a vacuum of at least 20 Å that separates periodic images of the nanowires. This is sufficient to ensure that the interaction between periodic images is negligible.

Under uniaxial stress conditions, the geometries were optimized for these hexagonal prism structures by using the classical MD simulations[30] technique implemented in the Large-scale Atomic/Molecular Massively Parallel Simulator (LAMMPS) package.[31] In this computational scheme, the ion–electron interaction was modeled by the Buckingham-type interatomic potential.[32] We consider [0001] orientation WZ ZnO nanowires as high quality single crystalline, with lattice constants $a = 3.249$ Å and $c = 5.206$ Å.[33]

After geometric construction, the ZnO nanowires are first equilibrated at a specified temperature and zero axial stress for 20 ps (a timestep of $\Delta t = 0.1$ fs is used), with periodic boundary conditions. In this work, isothermal-isobaric (NPT) ensemble is used, and the pressure is atmospheric pressure. To ensure the equilibrium, we obtained the total energy versus simulation time at 300 K. Figure 1(b) shows a relationship between the total energy and simulation time (or time steps) for ZnO nanowires at 300 K. This result indicates that 2.0×10^5 MD steps are sufficient to reach the steady state for the total energy, and similar results hold true for all ZnO nanowires studied in this work.

After that, approximation to quasi-static tensile loading in each deformation increment is achieved in two steps, and a schematic representation of the system is shown in Figure 1(a). Firstly, a special strain $\Delta\varepsilon_z$ is applied to boundary atoms along the [0001] orientation. This is followed by equilibration of the entire structure for 3 ps with boundary atoms fixed at their current positions. In general, the simulation procedure for the tensile deformation is similar to that used in our previous work.[34] Finally, stress–strain curves of ZnO nanowires are obtained by plotting the relationship between strain and the corresponding stress, and then the Young's moduli are obtained from the slope of the linear portion of such stress–strain curves.

To verify the accuracy of our current computational method, stress versus strain curves in the [0001]-oriented crystal of bulk ZnO have been calculated by using the above methodology at 300 K, and they are shown in Figure 2. The Young's modulus can be obtained by

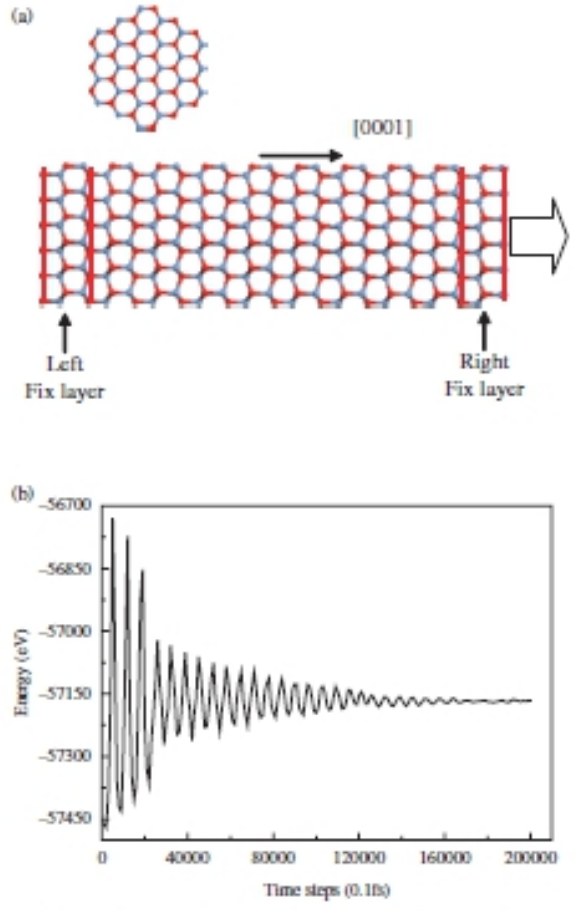

Fig. 1. (a) A schematic representation of the simulated ZnO NWs. (b) Convergence dynamics to reach the steady state for ZnO NWs at 300 K.

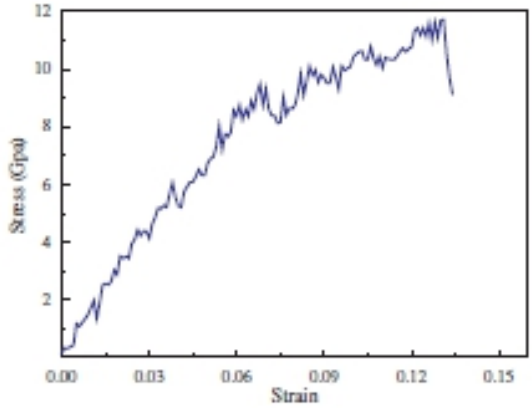

Fig. 2. Stress versus strain curves for bulk ZnO with [0001] crystal orientation at 300 K.

RESEARCH ARTICLE

Table I. Calculated Young's modulus compared to experimental and other theoretical values for single-crystal ZnO.

ZnO	Young's modulus (GPa)
Kobiakov[35]	140
Kucheyev[36]	111.2 ± 4.7
Coleman[37]	143 ± 6
Navamathavan[38]	140 ± 3
Jian[39]	112.5 ± 8.4
Gadzhiev[40]	123
Qi[41]	144.2
Kulkarni[19]	119.7
This work	142.12

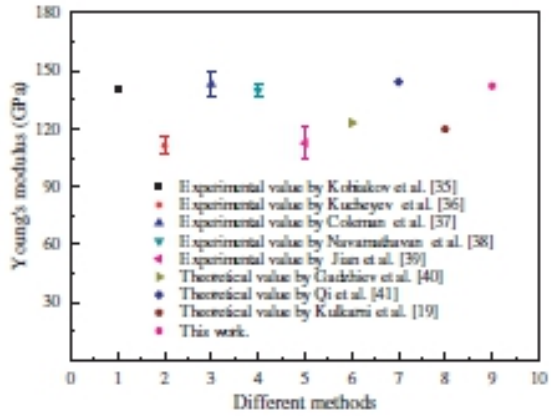

Fig. 3. Calculated Young's modulus compared to experimental and other theoretical values for bulk single-crystal ZnO.

calculating the slope of the straight line in the elastic region (up to 3%). As shown in Table I and Figure 3, the calculated Young's modulus agrees perfectly well with experimental and other theoretical data.[19, 35-41] Therefore, this methodology and parameters are appropriate, and the mechanical properties from our calculations are reliable. We also take note of similar methodologies applied successfully to the analysis of the mechanical behaviors of several other nanostructures.[19, 42-44]

3. RESULTS AND DISCUSSION

3.1. Strain Rate Effect on Mechanical Properties

To analyze strain rate effects on mechanical properties, stress–strain curves of ZnO nanowires in the range of strain rate from 0.001 to 0.03 ps^{-1} with cross-sectional areas of 3 nm^2 have been investigated at 300 K.

Figure 4 shows the relationship between computed stresses and strains under different strain rates conditions. It can be seen that the stress–strain curves at these strain rates overlap with each other until the nanowire yields. Entire ZnO nanowires Young's module computed are less affected by strain rates within the strain rates range studied in this work. In particular, the Young's modulus is

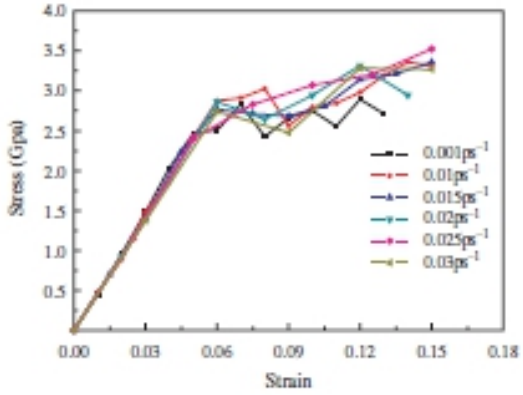

Fig. 4. Stress–strain responses with strain rate ranging from 0.001 to 0.03 ps^{-1} at cross sectional area of 3 nm^2 and temperature of 300 K.

49.7 GPa. Ultimately, it is also noted that the Young's modulus of ZnO nanowires determined here is lower than that of bulk ZnO (142.12 GPa).

3.2. Temperatures Effect on Mechanical Properties

Temperature has a significant effect on the mechanical properties of nanowires, so low dimensional nanostructures with different temperatures show distinctive deformation behaviors under loading.[45] In this work, the effect of temperature on deformation is also analyzed using nanowires 3 nm^2 in lateral dimensions. In this analysis, the strain rate has been 0.001 ps^{-1}, and the temperature has been ranging from 200 K to 1600 K to quantify the effect of temperature on the behavior.

Figure 5 shows the responses of different temperatures in stress–strain. The linear elastic stages of deformation and the stress drop associated with the transformation are clear at all temperatures. A significant dependence on temperature is observed. To analyze in detail, temperature dependent Young's moduli have been determined from the corresponding stress–strain responses by using a linear

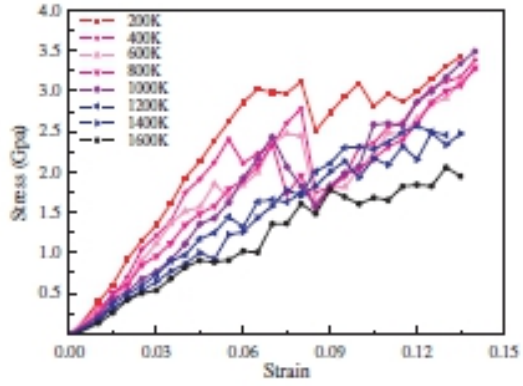

Fig. 5. Stress–strain responses with temperature ranging from 200 to 1600 K for ZnO NWs with cross sectional area of 3 nm^2.

RESEARCH ARTICLE

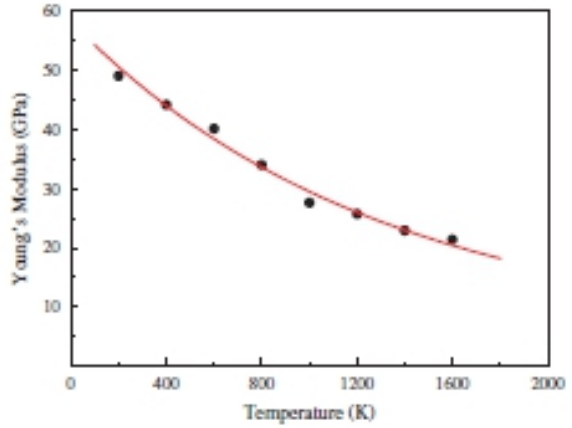

Fig. 6. Variations of the Young's modulus with temperature increasing from 200 to 1600 K; ZnO NWs cross-sectional area is 3 nm^2.

regression, as shown in Figure 6. The measured values of the Young's modulus of ZnO NWs are shown as a function of the temperature in Figure 6. All details on Young's modulus values are summarized in Table II. It can be seen from Table II, as the temperature increases from 200 K to 1600 K, the Young's modulus decreases 56.4% from 49.1 GPa to 21.4 GPa.

In the following, we further computed total energy as a function of strain at different temperatures to understand the mechanism of Young's modulus decrease monotonically with temperature. The total energy as a function of strain is shown in Figure 7. With temperature increasing from 200 K to 1600 K, the total energy increases, and then the structural stability decreases. This may account for the Young's modulus decrease monotonically with temperature.

3.3. Cross-Sectional Area Effect on Mechanical Properties

Then, the effect of cross-sectional area size on deformation is also analyzed at the temperature of 300 K. As the deformation progresses, the strain rate has been 0.001 ps^{-1} and the cross sectional areas analyzed here have been ranging from 1.1 nm^2 to 20.0 nm^2. Figure 8 shows the stress–strain curve dependent on the cross sectional area of ZnO NWs. It can be seen that the Young's modulus increase dramatically with increasing cross sectional area, but the values are lower than that of bulk structure. At 300 K, the calculated mechanical properties of ZnO NWs with cross sectional area are also summarized in Table III. Specifically,

Table II. Calculated mechanical properties at different temperature conditions for ZnO NWs' cross-sectional areas of 3 nm^2.

Temperature (K)	200	400	600	800	1000	1200	1400	1600
Young's modulus (GPa)	49.1	44.2	40.16	34.07	27.67	25.74	22.93	21.38

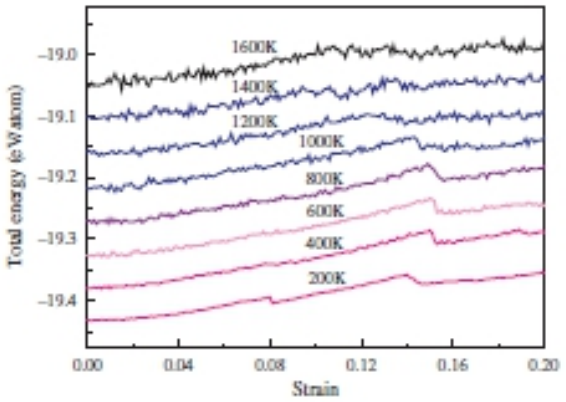

Fig. 7. Total energy curves as a function of strain at different temperatures.

as shown in Table III, as the cross sectional area increases from 1.1 to 20.0 nm^2, an increase of 394.5% in yield strength and 362.7% in Young's modulus is observed, respectively. Figures 9(a) and (b) show the relationship of the Young's modulus and yield strength with cross sectional area. As can be seen, the Young's modulus of ZnO NWs increases with increasing cross sectional area. It is expected that, as cross sectional area increases further, the Young's moduli will eventually approach their respective values of bulk ZnO ($E_{bulk} = 142.12$ GPa).

The following exponential formula can be fitted to describe the relationship between the cross sectional area and the Young's modulus, namely

$$E = 7.0542 - 6.567 \exp\left(\frac{A}{8.667}\right)$$

where A is the cross sectional area (in nm^2), E is the Young's modulus (in GPa).

The above trend can be explained by the state of stress in the stable structure of ZnO NWs. Since ZnO NWs

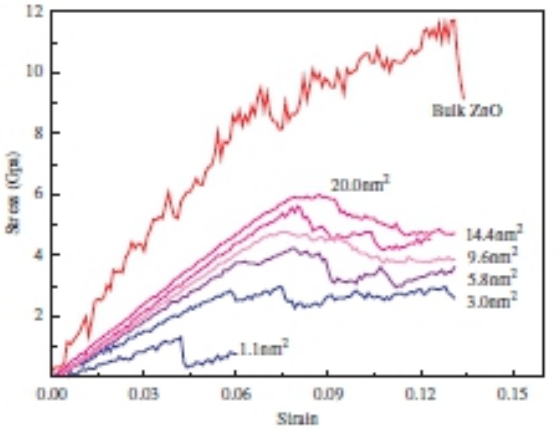

Fig. 8. Stress–strain curves with ZnO NWs cross sectional areas ranging from 1.1 nm^2 to 20.0 nm^2 at 300 K.

RESEARCH ARTICLE

Table III. Variations of mechanical properties of ZnO NWs with cross sectional area ranging from 1.1 to 20.0 nm² at temperature of 300 K.

Cross sectional area (nm²)	Yield strength (GPa)	Young's modulus (GPa)	Fracture strength (GPa)	Fracture strain
1.1	1.28	30.71	0.76	0.06
3.0	2.81	49.69	2.66	0.13
5.8	3.77	62.80	3.47	0.132
9.6	4.73	73.42	3.86	0.131
14.4	5.54	81.13	4.5	0.123
20.0	6.33	90.49	4.7	0.13
Bulk ZnO	11.37	142.12	10.54	0.127

are high quality single crystals with no defects, it is expected that such a phenomenon of size dependence may originate from the stress in the ZnO nanowires. Surface stress is inversely related to the cross sectional area of the nanowires.[19,46] When the cross sectional area is sufficiently large, the surface stress induced compressive pressure is very small and the surface effects are insignificant, and then the properties approach that of the bulk.

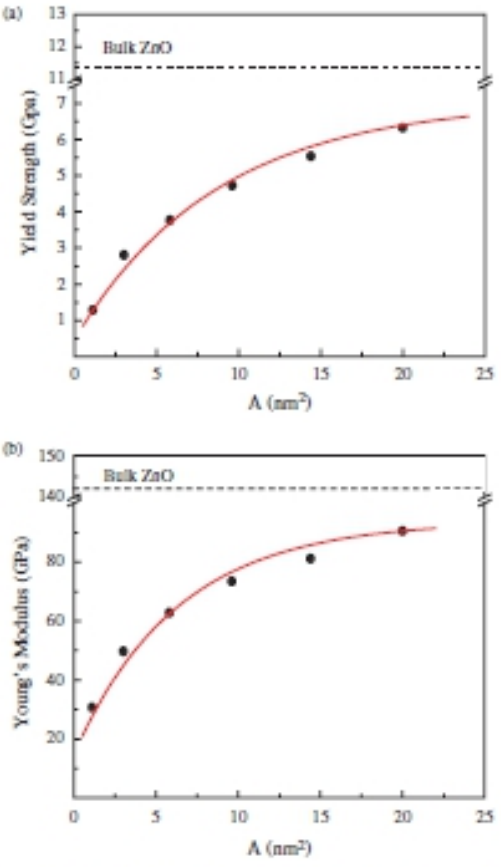

Fig. 9. Variations of the yield strength (a) and Young's modulus (b) with the inverse of ZnO NWs cross sectional area increasing from 1.1 to 20.0 nm².

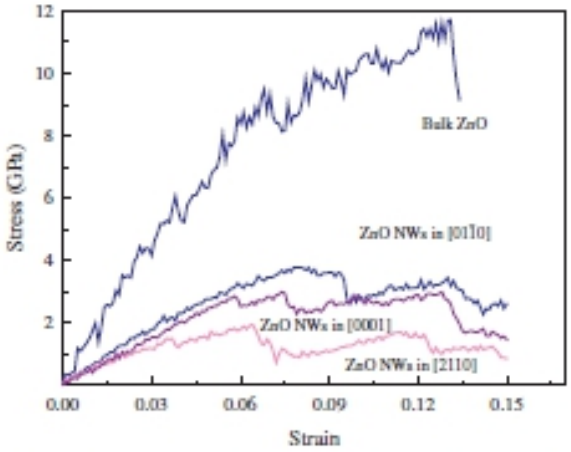

Fig. 10. Stress–strain curves with ZnO NWs in [01$\bar{1}$0], [0001] and [2$\bar{1}\bar{1}$0] crystal orientations at 300 K. Also shown are data of bulk ZnO computed in this simulation.

3.4. Orientation Effect on Mechanical Properties

Furthermore, to analyze orientation dependence, we calculate the tensile strains of ZnO NWs with cross-sectional areas 3 nm² at 300 K. Three crystal orientations have been considered, that is [01$\bar{1}$0], [0001] and [2$\bar{1}\bar{1}$0] crystal orientations. The relationships between crystal orientations and stress–strain responses for these three crystal orientations ZnO NWs are shown in Figure 10. It is indicated that different orientations show distinct deformation behaviors under loading.

For [0001] crystal orientation ZnO NWs, the yield strength is 2.8 GPa and the Young's modulus is 49.7 GPa. However, for [2$\bar{1}\bar{1}$0] crystal orientation ZnO NWs, Young's modulus has a 26.7% drop and the yield strength has a 49.4% drop, respectively. For [01$\bar{1}$0] crystal orientation ZnO NWs, it will amount for 19.8% in Young's modulus and 35.8% in yield strength increase respectively. In particular, Young's modulus in [01$\bar{1}$0] crystal orientation is significantly larger than that of in [2$\bar{1}\bar{1}$0] and [0001] crystal orientations. It has also indicated that Young's moduli in all ZnO NWs considered here are lower than those of bulk ZnO.

4. CONCLUSIONS

In conclusion, we have used molecular dynamics simulations to investigate mechanical properties of ZnO nanowires with [0001]-oriented. Our MD simulations predicted that with strain rates ranging from 0.001 to 0.03 ps^{-1}, strain rates have almost no effect on Young's modulus. Our simulations also demonstrated that the Young's moduli are decreasing with increasing temperature from 200 K to 1600 K. Moreover, in contrast to recent reports, it is demonstrated that, at the same temperature conditions, the yield strength and Young's modulus increases dramatically

RESEARCH ARTICLE

with increasing cross sectional area, gradually approaching the value of bulk single-crystal ZnO. Finally, orientation dependent ZnO nanowires mechanical properties have been studied. In particular, we found that Young's modulus in $[01\bar{1}0]$ crystal orientation is significantly larger than that of in $[2\bar{1}\bar{1}0]$ and [0001] crystal orientations.

Acknowledgments: This work was supported by the National Natural Science Foundation of China (Grants 50772018, 50402025) and the Program for New Century Excellent Talents in Chinese Universities (NCET-07-0139). Roderick Melnik acknowledges the support from the NSERC and CRC program. This work was made possible by the facilities of the Shared Hierarchical Academic Research Computing Network (SHARCNET), Canada.

References

1. Y. Xia, P. Yang, Y. Sun, Y. Wu, B. Mayers, B. Gates, Y. Yin, F. Kim, and H. Yan, *Adv. Mater.* 15, 353 (**2003**).
2. B. P. Zhang, N. T. Binh, and Y. Segawa, *Appl. Phys. Lett.* 84, 586 (**2004**).
3. U. Ozgur, Y. I. Alivov, C. Liu, A. Teke, M. A. Reshchikov, S. Dogan, V. Avrutin, S. J. Cho, and H. Morkoc, *J. Appl. Phys.* 98, 041301 (**2005**).
4. C. Tusche, H. L. Meyerheim, and J. Kirschner, *Phys. Rev. Lett.* 99, 026102 (**2007**).
5. Y. Wang, X. Fan, and J. Sun, *Mater. Lett.* 63, 350 (**2009**).
6. X. Y. Kong, Y. Ding, R. Yang, and Z. L. Wang, *Science* 303, 1348 (**2004**).
7. P. X. Gao, Y. Ding, W. Mai, W. L. Hughes, C. Lao, and Z. L. Wang, *Science* 309, 1700 (**2005**).
8. Z. W. Pan, Z. R. Dai, and Z. L. Wang, *Science* 291, 1947 (**2001**).
9. M. H. Zhao, Z. L. Wang, and S. X. Mao, *Nano Lett.* 4, 587 (**2004**).
10. Y. Huang, J. He, Y. Zhang, Y. Dai, Y. Gu, S. Wang, and C. Zou, *Journal of Materials Science* 41, 3057 (**2006**).
11. J. Duan, X. Huang, and E. Wang, *Mater. Lett.* 60, 1918 (**2005**).
12. I. Shalish, H. Temkin, and V. Narayanamurti, *Physical Review B* 69, 245401 (**2004**).
13. G. S. Wu, T. Xie, X. Y. Yuan, Y. Li, L. Yang, Y. H. Xiao, and L. D. Zhang, *Solid State Commun.* 134, 485 (**2005**).
14. Z. L. Wang and J. Song, *Science* 312, 242 (**2006**).
15. B. Wen and R. Melnik, *Appl. Phys. Lett.* 92, 261911 (**2008**).
16. Z. Yang, B. Wen, R. Melnik, S. Yao, and T. Li, *Appl. Phys. Lett.* 95, 192101 (**2009**).
17. B. M. Wen, J. E. Sader, and J. J. Boland, *Phys. Rev. Lett.* 101, 175502 (**2008**).
18. X. Wang, J. Song, J. Liu, and Z. L. Wang, *Science* 316, 102 (**2007**).
19. A. J. Kulkarni, M. Zhou, and F. J. Ke, *Nanotechnology* 16, 2749 (**2005**).
20. A. J. Kulkarni, M. Zhou, K. Sarasamak, and S. Limpijumnong, *Phys. Rev. Lett.* 97, 105502 (**2006**).
21. X. D. Bai, P. X. Gao, Z. L. Wang, and E. G. Wang, *Phys. Rev. Lett.* 82, 4806 (**2003**).
22. K. Yum, Z. Wang, A. P. Suryavanshi, and M. F. Yu, *J. J. Appl. Phys.* 96, 3933 (**2004**).
23. J. H. Song, X. Wang, E. Riedo, and Z. L. Wang, *Nano Lett.* 5, 1954 (**2005**).
24. M. H. Zhao, C. B. Jiang, S. X. Li, and S. X. Mao, *Mater. Sci. Eng. A* 409, 223 (**2005**).
25. H. Ni and X. D. Li, *Nanotechnology* 17, 3591 (**2006**).
26. W. Mai and Z. L. Wang, *Appl. Phys. Lett.* 89, 073112 (**2006**).
27. C. Q. Chen, Y. Shi, Y. S. Zhang, J. Zhu, and Y. J. Yan, *Phys. Rev. Lett.* 96, 075505 (**2006**).
28. L. Zhang and H. C. Huang, *Appl. Phys. Lett.* 89, 18311 (**2006**).
29. G. Wang and X. Li, *Appl. Phys. Lett.* 91, 231912 (**2007**).
30. S. J. A. Koh, P. H. Lee, and Q. H. Cheng, *Physical Review B* 72, 085414 (**2005**).
31. S. J. Plimpton, R. Pollock, and M. Stevens, Particle-mesh Ewald and rRESPA for parallel molecular dynamics simulations, *Proc. Eighth SIAM Conference on Parallel Processing for Scientific Computing, Machines*, MN (**1997**).
32. D. J. Binks and R. W. Grimes, *J. Am. Ceram. Soc.* 76, 2370 (**1993**).
33. Y. Zhang, L. Wang, X. Liu, Y. Yan, C. Chen, and J. Zhu, *J. Phys. Chem. B* 109, 13091 (**2005**).
34. J. Guo, B. Wen, R. Melnik, S. Yao, and T. J. Li, *Diamond Relat. Mater.* 20, 551 (**2011**).
35. I. B. Kobiakov, *Solid State Commun.* 35, 305 (**1980**).
36. S. O. Kucheyev, J. E. Bradby, J. S. Williams, C. Jagadish, and M. V. Swain, *Appl. Phys. Lett.* 80, 956 (**2002**).
37. V. A. Coleman, J. E. Bradby, C. Jagadish, P. Munroe, Y. W. Heo, S. J. Pearton, D. P. Norton, M. Inoue, and M. Yano, *Appl. Phys. Lett.* 86, 203105 (**2005**).
38. R. Navamathavan, K. K. Kim, D. K. Hwang, S. J. Park, J. H. Hahn, T. G. Lee, and G. S. Kim, *Appl. Surf. Sci.* 253, 464 (**2006**).
39. S. R. Jian, *J. Alloys Compd.* 494, 214 (**2010**).
40. G. G. Gadzhiev, *Teplofizika Vysokikh Temperatur* 41, 877 (**2003**).
41. J. S. Qi, D. N. Shi, and B. L. Wang, *Computational Materials Science* 46, 303 (**2009**).
42. S. K. R. S. Sankaranarayanan, V. R. Bhethanabotla, and B. Joseph, *Physical Review B* 76, 134117 (**2007**).
43. S. Inoue and Y. Matsumura, *Chem. Phys. Lett.* 469, 125 (**2009**).
44. S. P. Ju, J. S. Lin, and W. J. Lee, *Nanotechnology* 15, 1221 (**2004**).
45. J. Wang, A. J. Kulkarni, F. J. Ke, Y. L. Bai, and M. Zhou, *Computer Methods in Applied Mechanics and Engineering* 197, 3182 (**2008**).
46. K. Gall, J. Diao, and M. L. Dunn, *Nano Lett.* 4, 2431 (**2004**).

RESEARCH ARTICLE

Molecular Dynamics Study on ZnO Nanowires Mechanical Properties: Strain Rate, Temperature and Size Dependent Effects

Authors: Guo, Jing; Wen, Bin; Melnik, Roderick

Source: Journal of Computational and Theoretical Nanoscience,

Volume 9, Number 12, December 2012 , pp. 2138-2143(6)

Publisher: American Scientific Publishers